NUMERICAL MODELING OF OOID SIZE AND THE PROBLEM OF NEOPROTEROZOIC GIANT OOIDS

DAWN Y. SUMNER AND JOHN P. GROTZINGER
Department of Earth, Atmospheric, and Planetary Sciences, Massachusetts Institute of Technology, Cambridge, MA 02139 USA

ABSTRACT: **Temporal variation in ooid size reflects important changes in physical and chemical characteristics of depositional environments. Two numerical models are used to evaluate the effects of several processes influencing ooid size. The first demonstrates that low supply of new ooid nuclei and high cortex growth rate each promote growth of large ooids. The second model demonstrates that high average water velocity and velocity gradient also enhance ooid growth.**

Several Neoproterozoic oolites contain unusually large ooids, some reaching diameters of up to 16 mm. While lower nuclei supply and higher ooid growth rate may have prevailed prior to the evolution of carbonate-secreting organisms, neither difference can explain the presence of giant ooids in Neoproterozoic deposits because Archean through Mesoproterozoic ooids rarely exceed 5 mm in diameter. In the presence of lower nuclei supply and higher growth rate, high average water velocity may have allowed growth of such large ooids. Higher average water velocity could have been due to a prevalence of carbonate ramps over rimmed shelves during Neoproterozoic time.

INTRODUCTION

Oolites have long been recognized as one of the most intriguing carbonate facies (Sorby 1879). The mineralogy, abundance, size, and sorting of ooids reflect the chemical and physical conditions of their depositional environment (Bathurst 1975; Davies et al. 1978; Heller et al. 1980). The diversity of ooids should be interpretable in terms of variations in these conditions.

Most discussions of secular variation in ooid characteristics focus on changes in mineralogy or abundance. The presence of aragonitic ooids at various times during the Phanerozoic may relate to high atmospheric carbon dioxide (Sandberg 1983; Sandberg 1985; Tucker 1992; Wilkinson et al. 1985), while the abundance of ooids seems to correlate with rate of sea-level change (Wilkinson et al. 1985). Except for Swett and Knoll (1989), few have considered secular variations in ooid size, although these changes may also reflect global sea-water chemistry and sedimentation styles. Work on modern ooids has led to several theories for size-limiting processes (Bathurst 1975; Carozzi 1989), but these processes have not been evaluated quantitatively or applied to size variation in ancient ooids.

The depositional environments of ooids can be better understood by using forward numerical models to test the sensitivity of average ooid size to various processes. Forward models are often designed to simplify systems by eliminating much of the complexity, but they provide valuable first-order information on the importance of individual processes. Although interpretations should be restricted to trends in model results due to variation in a single variable, these models can help identify important processes and suggest approaches for further modeling.

Here we present two numerical models. The first demonstrates the dependence of ooid size on cortex growth rate, supply of new ooid nuclei, and reworking of ooids by storms. The second relates average water agitation and velocity gradient to ooid size. Neither accurately reflects all of the growth processes affecting final ooid size, but they are useful for determining whether individual processes can account for observed variations in ooid size.

Neoproterozoic oolites provide an interesting application for model results. While most modern and Phanerozoic marine ooids are less than 1 mm in diameter and few deposits contain ooids larger than 2 mm in diameter (Amsden and Barrick 1986; King and Chafetz 1983; Milliman and Barretto 1975), several Neoproterozoic carbonate platforms contain abundant giant ooids (Table 1). (By definition, ooids are less than 2 mm in diameter (Peryt 1983). However, in this paper we use the term "giant ooids" rather than "pisoids" for grains larger than 2 mm to emphasize the similarity in grain genesis.) For example, the Akademikerbreen Group in Spitsbergen contains 400 m of section with abundant ooids 4–9 mm in diameter and with a maximum ooid diameter of 14 mm (Knoll and Swett 1990; Swett and Knoll 1989). These giant ooids are not just large nuclei with thin superficial coatings, but silt-sized nuclei with anomalously thick cortices. Several Neoproterozoic oolites have similar size distributions, although except for the Katakturuk Dolomite in Alaska (Blodgett et al. 1986; R.K. Goldhammer, personal communication 1992), none of these other successions contain as great an abundance of giant ooids. By combining model results and geological considerations, several mechanisms can be eliminated as the sole cause of the growth of these giant ooids.

CONTROLS ON OOID SIZE

Several processes affect ooid size, including burial rate, growth rate, mobility, and abrasion of ooids.

Burial Rate.—Although Bathurst (1975) stated that rate of ooid burial is the ultimate constraint on size, little effort has been made to relate it to the size of modern ooids. Ooid burial rate can be equated to supply of new ooid nuclei: rapid supply of nuclei should lead to rapid burial of small ooids, whereas low supply should leave ooids on the growth surface long enough to develop thick cortices. The two extreme cases are an exceedingly low sedimentation rate, for which the ooids continue to grow until they are too large to be overturned for symmetrical growth, and a sedimentation rate so high that none of the incoming nuclei are coated prior to burial. Intermediate nuclei supply leads to growth of intermediate-size ooids.

Supply of ooid nuclei varies with location and time. The evolution of carbonate-secreting and pellet-forming organisms near the Precambrian–Cambrian boundary is particularly important. Since most Phanerozoic ooids are nucleated on pellets or shell fragments (Bathurst 1975), ooid nucleation rates could have been much lower prior to volumetrically important production of these grains.

Growth Rate.—High growth rates produce larger ooids than low rates for a given growth time, as discussed by Swett and Knoll (1989) for Neoproterozoic giant ooids. Growth rate is controlled by the saturation state of sea water, kinetic factors inhibiting or promoting precipitation, degassing of carbon dioxide, delivery of fresh chemical species to the surface of the ooid, and ease of precipitation on the ooid surface. Degassing of carbon dioxide and supply of fresh chemical species depend on local hydraulic conditions, whereas ease of precipitation depends on ooid burial history and organic coatings (Davies et al. 1978; Weyl 1967). Specific effects of these processes are complex and not well understood, but all factors affecting ooid growth rate can be combined into a single variable that represents the average growth rate for ooids in the system. Change in growth rate may be due to any one of these factors and does not necessarily represent a change in carbonate saturation state.

Agitation.—Carozzi (1989) concluded that ooid growth ceases once ooids become too large to be mobilized under local conditions; this implies that mobility or agitation is the primary control on ooid size. Bathurst (1975) noted the presence of ooids in very low-energy environments such as southeast Bimini Lagoon and concluded that regular agitation is not required for growth. He did report, however, that greater ooid mobility

JOURNAL OF SEDIMENTARY PETROLOGY, VOL. 63, NO. 5, SEPTEMBER, 1993, P. 974–982
 0022-4472/93/0063-974/$03.00

TABLE 1.—*Occurrences of ooids > 2 mm in diameter*

Location	Size (mm)	Environment	Comments	Reference
Late Archean				
Carawine Dol., Australia	≤ 6	low energy platform	most ≤ 1 mm	Simonson and Jarvis, in press; Simonson et al. 1993
Boomplaas Fm., South Africa	≤ 5	ramp	–	Beukes 1983
Reivilo Fm., South Africa	≤ 3	ramp	most ≤ 1.5 mm	personal observation; Truswell and Eriksson 1973
Frisco Fm., South Africa	≤ 18	condensed zone of rimmed shelf	most ≤ 5 mm	personal observation
Paleoproterozoic				
Nabberu Basin, Australia	≤ 4	reef	size from photo	Hall and Goode 1978
Rocknest Fm., Northwest Territories	≤ 2.5	back reef	–	personal observation; Grotzinger and Read 1983
Mesoproterozoic				
Belt Supergr., Montana	≤ 2.5	–	most ≤ 1.4 mm	Tucker 1984
Neoproterozoic				
Eleonore Bay Gr., Greenland; Akademiderbreen and Raoldtoppen Grs., Svalvard	1–14	ramp	most 4–9 mm	Swett and Knoll 1989
Beck Spring Fm., California	≤ 10	ramp	–	personal observation; Gutstadt 1968
Trezona Fm., Australia	≤ 16	subtidal barrier	–	Singh 1987
Yellowhead Platform, Alberta	≤ 4.5	ramp	–	Teitz and Mountjoy 1989
Katakturuk Dol., Alaska	4+	active shelf margin	most > 4 mm	R. Goldhammer, personal communication; Clough et al. 1988
Wilhite Fm., Smokey Mtns.	≤ 5	sediment gravity flows	–	personal observation
Reed Dol., California	≤ 5	–	–	C. Summa, personal communication
Johnnie Fm., California	≤ 12	in breccia blocks	–	C. Summa, personal communication
Bitter Springs Fm., Australia	≤ 2	intracratonic basin	"peloids" also present	Southgate 1989
Cambrian				
Riley Fm., Texas	≤ 5	ramp (?)	98% < 1 mm	King and Chafetz 1983
Nolichucky Fm., Virginia	≤ 4	shallow ramp	largest coat shell fragments	Markello and Read 1981
Ordovician				
Keel Fm., Oklahoma	≤ 5	shallow seaways	most < 2 mm	Amsden and Barrick 1986
Devonian				
Portilla Fm., Spain	≤ 5	ramp	size from photos	Reijers and ten Have 1983
Carboniferous				
Plattsburg Limestone, Kansas	≤ 3	–	–	Wilkinson et al. 1984
Kohlenkalk, Germany	≤ 4	–	size from photo	Richter 1983
Jurassic				
Calcare Massiccio Fm., Italy	≤ 3.5	–	size from photos	Ciarapica and Passeri 1983
Quaternary				
Amazon Shelf, Brazil	≤ 1	outer continental shelf	rare > 2 mm	Milliman and Barretto 1975

seems to result in thicker cortex layering and possibly faster growth rates. Irrespective of whether regular agitation is necessary for ooid growth, most indications are that agitation promotes growth of large ooids. An agitated environment is also necessary for sorting of ooids and production of winnowed deposits of large ooids.

Abrasion.—Abrasion may be a limiting factor in the size of modern ooids. On the basis of the development of spherical ooids from irregular and platy nuclei, Bathurst (1975) suggested that abrasion is the main control on maximum ooid size. For a sphere to develop, the cortex must grow more quickly on surface depressions than on protrusions, possibly due to enhanced abrasion on projecting parts of the ooid. Other evidence for the importance of abrasion is its effect on ooid microtextures: small ooids and the inner regions of large ooids are often radial, whereas the outer coatings on large ooids consist of tangentially oriented crystals. This change is probably due to crystal reorientation from increased impact force or frequency (Heller et al. 1980; Medwedeff and Wilkinson 1983) and may reflect an increase in abrasion. Lamina thickness tends to decrease outward in the cortex, also suggesting an increase in mass lost by abrasion (Bathurst 1975; Medwedeff and Wilkinson 1983).

The argument that abrasion limits ooid size is based on the rapid increase of mass loss due to abrasion with increasing ooid size (Bathurst 1975). The mass loss per impact $\Delta m_{abrasion}$ is proportional to the force of the impact F_{impact} (see list of variables at end of paper):

$$\Delta m_{abrasion} = KF_{impact} \tag{1}$$

where K is a factor that describes the strength of the ooid and determines the actual mass loss for a given force. Force is related to both the mass of the ooid and the deceleration a the ooid experiences during the collision:

$$\Delta m_{abrasion} = K\rho\frac{4}{3}\pi r^3 a \tag{2}$$

where ρ is ooid density and r is ooid radius. From this, the mass loss per unit time is

$$\Delta m_{abrasion}\frac{I}{t} = K\rho\frac{4}{3}\pi r^3 a\frac{I}{t} \tag{3}$$

where I is the number of impacts in time t.

Rate of mass loss due to abrasion increases as the cube of the ooid radius (Eq 3), all other variables constant:

$$\frac{\Delta m_{abrasion}}{t} \propto r^3 \tag{4}$$

In contrast, the rate of increase $\Delta m_{growth}/t$ in ooid mass due to growth is proportional to the surface area of the ooid:

$$\frac{\Delta m_{growth}}{t} \propto 4\pi r^2 \tag{5}$$

Eqs 4 and 5 show that abrasion-related mass loss increases more quickly with ooid size than mass gain due to growth. Thus, as ooids become larger, abrasion becomes more important and may eventually limit further growth.

Although the relationship between mass loss and growth rate relative to ooid radius is simple, it is difficult to quantify ooid size in a numerical model, and without quantifying ooid radius there are no constraints for choosing the magnitude of abrasion. A large value eliminates all ooid growth while a small value has no effect on ooid size, and an intermediate value limits ooid size to any value of choice. It is thus essential to quantify ooid size if abrasion is to be included in the numerical model. To quantify ooid sizes, it is necessary to know realistic water velocity, nucleation rate, growth rate, and burial effects on growth rate. These complications, together with the many time steps required, greatly increase the necessary computational power.

Abrasion-related mass loss depends also on the deceleration a of ooids during impacts, the number of impacts per unit time I/t, and the factor K that reflects bold strength. These relationships are complex. For example, the mode of transport of ooids is important because ooids in traction experience many more forceful collisions than those in suspension. The number and force of collisions depend on water velocity, size of individual ooids, and size distribution of ooids in the system. The factor K describing mass loss depends on ooid strength, i.e., integrity, alignment, and mineralogy of the crystals, as well as effects such as grain boring, organic coatings, and recrystallization. While some of these effects may be small, their importance in determining abrasion rates has not been constrained.

Even though abrasion is an important process affecting ooid growth, it does not vary independently of other size-controlling factors. The physical relationships linking abrasion to ooid size and impact forces are independent of time. Thus, abrasion alone cannot cause temporal variation in ooid size: it can only limit ooid size under specific conditions. For example, if growth rates are high, the upper size limit from abrasion is large. If the supply of ooid nuclei is also high, ooids are buried before they reach the maximum size allowed by abrasion. In this case, nuclei supply controls ooid size and abrasion has little effect. In other circumstances, e.g., times with low growth rates, abrasion may be the most important size-controlling factor, but only because other processes are not strong enough to overcome its effects. Thus, constraints on ooid size can be modeled without including abrasion if only the qualitative trends in ooid size are interpreted and little emphasis is placed on the absolute sizes. This is particularly true for tests of nuclei supply and growth rate, both of which do not affect the rate of abrasion for a given ooid size. Analyses of the effects of agitation are more sensitive to the absence of abrasion in the models, because stronger agitation may increase abrasion rates by increasing the number and force of collisions. However, a decrease in abrasion rate is also possible if the number of ooids in suspension increases greatly. The dependence of ooid size on agitation derived computationally should thus be interpreted with caution and compared carefully to field evidence.

MODELS OF OOID GROWTH

Two models for the growth of ooids are presented here. The first demonstrates that lower nucleation rate and higher growth rate lead to larger ooids and that reworking by storms does not affect ooid size. The second model sorts ooids hydraulically as they form, simulating processes on an ooid shoal. This model demonstrates that high water velocity and steep velocity gradient enhance the growth of large ooids and improve sorting.

Growth Model

The growth model represents a one-dimensional sedimentary column of ooids (Fig. 1). No ooids can leave the system laterally, and only a preset number of ooid nuclei can enter. Four bins are defined in the model. Ooids in the growth bin are reworked continuously by current activity and are actively growing. The deposition bin contains ooids that have been deposited but not buried deeply, while the burial bin contains ooids that are buried too deeply to be exhumed. The return bin holds exhumed ooids temporarily before they are redeposited. Ooids are individually identified until they enter the burial bin, where they are tabulated by size.

The first step in the algorithm is to introduce ooids to the return bin by mobilization of ooids in the deposition bin and the growth bin. The frequency-depth distribution used for erosional events ("storms") is

$$f = e^{-D/\lambda} \tag{6}$$

where f is frequency of erosion to depth D and λ is a scaling factor for the average exhumation depth. An exponential decay function makes deeper erosional events much less frequent than shallower events. Results are insensitive to the exact form of the dependence. A random depth was generated using $D = -\lambda \ln(R)$, where R is a random number between 0 and 1. This equation transforms an evenly distributed random-number generator into one producing the exponential distribution in Eq 6 (Press et al. 1988). All ooids above the exhumation depth are eroded and placed in the return bin regardless of size. If the calculated depth of erosion is less than the depth D_{growth} of the growth bin, all ooids in the growth bin are exhumed. This ensures that ooids above D_{growth} are continuously reworked, reflecting daily processes. Ooids below the depth D_{max} at which $f < 0.001$ in Eq 6 are considered permanently buried, defining the top of the burial bin. During the first time step of the model, no ooids are present for erosion, so none are placed in the return bin. In subsequent time steps, all ooids are exhumed if there are not enough to fill the growth bin.

After the ooids are exhumed, new ooid nuclei are added to the return bin. A set number of grains are added with a specified radius. Since these grains are added to the system before deposition and growth of exhumed ooids, they can be deposited without any oolitic coatings.

Next, the ooids in the return bin are randomly deposited. Random deposition is used for two reasons: (1) grainstones can be unsorted under very rapid sedimentation rates, and (2) in a one-dimensional model the use of size-dependent deposition eliminates all effects of erosion on ooid size *a priori*. When the largest ooids are deposited first, a uniform size is preserved and reworking of ooids does not change their distribution within the model. Unsorted deposition is also consistent with other assumptions, such as lack of effects of lateral transport and grain size in exhumation of ooids.

Deposited ooids are stacked randomly in the growth bin. Once all ooids are deposited, the depth is calculated down from the top for all ooids not in the burial bin. Ooids above D_{growth} are retained in the growth bin. Those between D_{growth} and D_{max} are placed in the deposition bin. Ooids below D_{max} are placed in the burial bin and their sizes are added to the previous tabulation.

After deposition, the radii of ooids remaining in the growth bin are increased by the specified amount of growth per time step. The model assumes that cortex growth occurs only during daily activity represented by the growth bin, and not during erosional events (in the return bin) or a combination of the two. This assumption is based on recognition that precipitation rates are slow (Weyl 1967), and significant growth of ooids seems unlikely during storms lasting a few days at most. Once ooids have grown, the process is repeated starting at the exhumation stage.

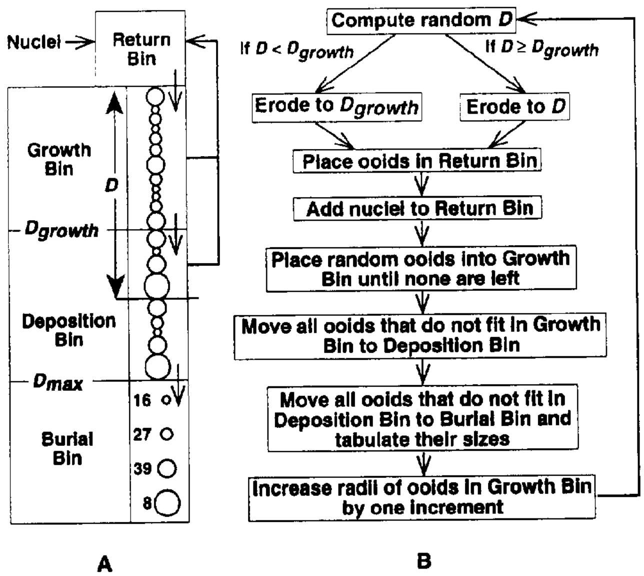

FIG 1.—Schematic representations of the growth model. **A)** A one-dimensional stack of ooids cycles from the return bin through the growth bin and deposition bin into the burial bin. Ooids are eroded down to a variable depth D in the deposition bin and placed in the return bin along with new ooid nuclei. Then they are randomly deposited into the growth bin. When the growth bin fills, ooids are placed in the deposition bin and then in the burial bin. Ooids in the burial bin are tabulated by size. **B)** Flow chart describing the specific steps of the program.

Output from the model consists of the final tabulation from the burial bin. These sizes represent equilibrium sizes and are independent of the number of time steps in the model provided that sufficient time has passed to bury a statistically significant number of ooids.

Results.—The growth model was tested for sensitivity to three parameters: supply of new nuclei, cortex growth rate, and depth-frequency distribution of exhumation events. During each set of runs all variables were held constant except for the one in question. New nuclei are assigned an initial radius of 10 units, and ooid sizes are reported as the thickness of the cortex. Cortex thicknesses do not change even if initial nuclei diameters are allowed to vary.

Nuclei Supply.—Ten model runs with 500 time steps, a growth rate of one unit per time step, and no exhumation below the growth bin are presented for each nuclei supply rate. The rate at which ooid nuclei are introduced to the system strongly influences the size of buried ooids. Cortex thickness increases rapidly at low supply rates (Fig. 2), demonstrating that low accumulation rates lead to larger ooids because of the longer residence time of ooids in the growth bin.

Variation (2σ) in size of deposited ooids for all runs (Fig. 2) demonstrates changes in ooid sorting with supply rate. (Note that the standard deviation of cortex thickness is much larger than the average cortex thickness.) Dispersion in deposited ooid size increases with decreasing supply rate, demonstrating an increase in the range of cortex thicknesses. At low nucleation rates, the largest ooid size increase considerably and the number of large ooids increases slightly, giving rise to less well sorted deposits. At high nucleation rates a large number of uncoated nuclei are deposited during each time step. These deposits are well sorted because ooids are quickly buried and seldom stay in the growth bin for more than a few time steps.

Growth Rate.—Ten model runs with 200 time steps, a nucleation rate of 10 nuclei per time step, and no exhumation below the growth bin are presented for each growth rate (Fig. 3). Cortex growth rate strongly influences the size of buried ooids (Fig. 3A). Average cortex thickness

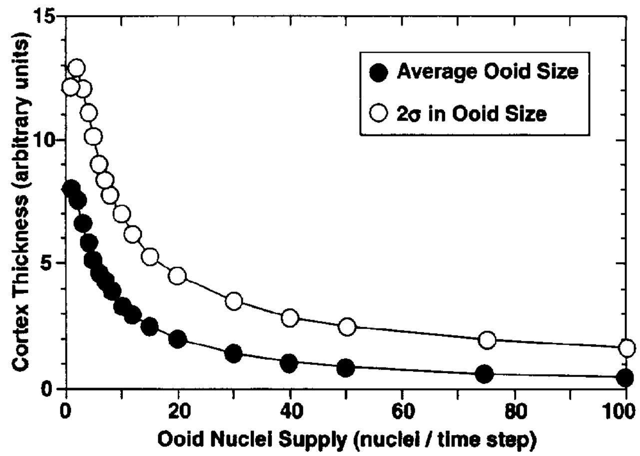

FIG 2.—Dependence of average cortex thickness and ooid sorting on ooid nuclei supply rate from the growth model. Average ooid size increases rapidly with decreasing nuclei supply. Two standard deviations (2σ) in ooid size represent the degree of sorting in deposited ooids and decreases rapidly with decreasing nuclei supply. At high nuclei supply rates, ooids are well sorted due to rapid burial; large ooids do not have a chance to form.

increases with growth rate, demonstrating that faster growth rates lead to larger ooids. The number of oolitic coatings decreases with increasing growth rate. Since the growth bin is defined as a depth rather than as a specific number of ooids, fewer large ooids fit in the bin than small ones. Thus, as average ooid size increases, the average time each ooid spends in the growth bin decreases, resulting in fewer coatings per ooid. Early burial causes the curve of growth rate vs. cortex thickness to deviate from a straight line (Fig. 3A), which is the expected relationship if the average growth time for each ooid remains constant.

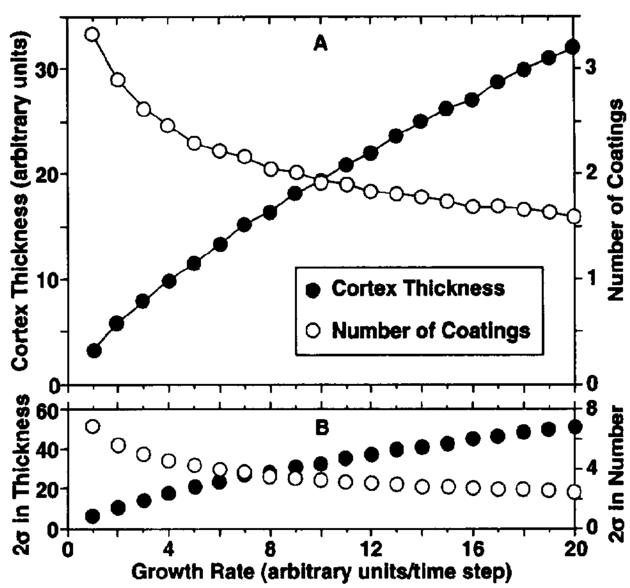

FIG 3.—Relationship between ooid size and growth rate from the growth model. **A)** Average cortex thickness increases rapidly with increasing growth rate while average number of coatings decreases, demonstrating that the increase in cortex thickness is due to increased growth per time step rather than to increased total growth time. **B)** Sorting of ooids (represented by 2σ in cortex thickness) decreases with increasing ooid size and growth rate even through the variation in the number of coating decreases.

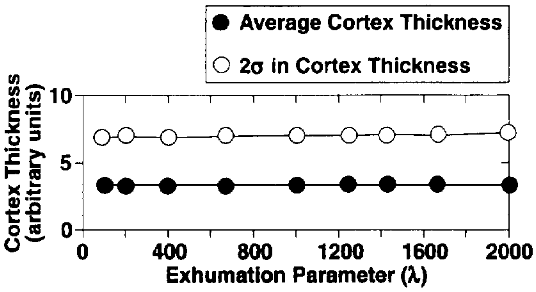

FIG 4.—Relationship between average cortex thickness and storm reworking from the growth model. Ooid size and sorting are independent of the extent of storm reworking.

The standard deviation of the size of deposited ooids varies substantially for both cortex thickness and number of coatings (Fig. 3B). As growth rate increases, variation in ooid size also increases, because of the greater size difference between ooids with slightly different growth times. This difference is demonstrated by the decrease in variation in number of coatings as variation in size increases. This implies that the decrease in sorting is due to the larger size difference between any given ooid and ooids that grow for one more time step.

Exhumation Frequency and Depth.—Ten model runs with 200 steps, growth rate of one unit per time step, and nucleation rate of 10 nuclei per time step are presented for each value of the exhumation parameter. The frequency of exhumation and redeposition of ooids during storms does not affect average ooid size (Fig. 4). No change in cortex thickness would be expected with increasing exhumation in a one-dimensional model with growth restricted to daily processes. The process of exhuming and redepositing ooids returns them to the growth bin but does not increase the average time they spend in the growth bin. For each group of ooids returned to the growth bin from burial, a corresponding thickness of ooids is buried and removed from an environment of active growth. Therefore burial frequency increases with return frequency. Without inclusion of sorting, enhancement of growth from agitation, or size-dependent erosion, reworking by storms does not affect ooid size in a one-dimensional model.

Sorting Model

The sorting model is a two-dimensional model consisting of a series of one-dimensional sedimentary columns between which ooids are transported (Fig. 5). The algorithm is modeled after a symmetric ooid shoal with no net transport direction. Unagitated columns are located at both ends of the model to trap ooids and keep them from leaving the system laterally. These columns grade linearly into more agitated columns in the center of the model, as on a shoal with water velocity increasing and water depth decreasing toward the peak.

The sorting model starts with random introduction of uniform ooid nuclei. Each column is assigned a certain probability P of receiving an ooid nucleus. This probability produces an average number $N = XP$ of nuclei N introduced to the whole system, where X is the total number of columns in the model. Nuclei are placed in the proper columns, burying any ooids previously in the columns.

Once nuclei are added, the water velocity for each column is calculated. The agitation for each column is defined as the water velocity in the previous column plus or minus the constant difference in velocity ΔV between neighboring columns. The water velocity also changes sinusoidally in time, mimicking tidal flow. For columns less than or equal to half the total number of columns, total water velocity $V(x)$ at time t is

$$V(x) = \Delta V x \cos(2\pi t/t_c) \qquad (7)$$

where x is the column label, numbered from left to right, and t_c is the

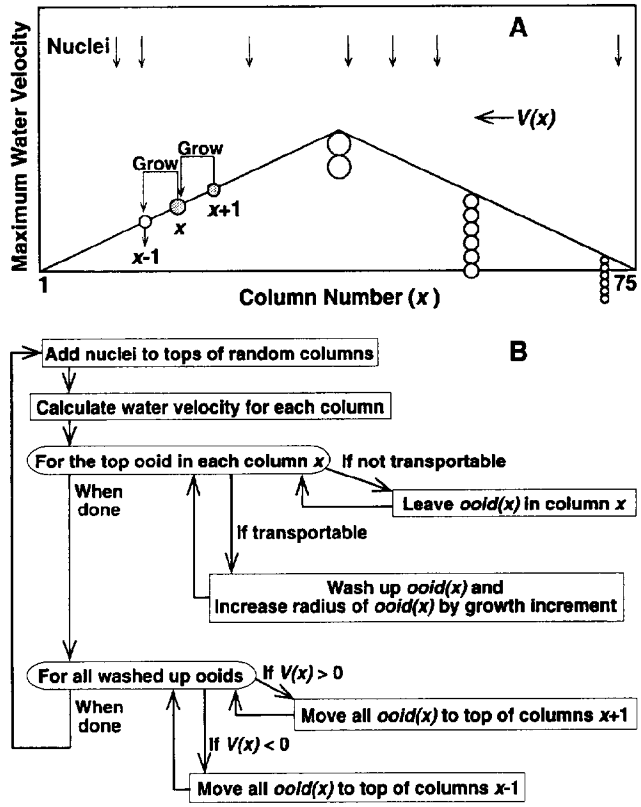

FIG 5.—Schematic representations of the sorting model. A) The model consists of a two-dimensional ooid shoal created by 75 columns between which ooids are transported. Nuclei are added randomly to the system. Then water velocity is calculated for each column with the magnitude increasing toward the center of the model. The magnitude and direction of velocity change sinusoidally in time, but at a given time the direction is the same throughout the model. All ooids that can be mobilized at a given time step are eroded, grown, and deposited simultaneously. Ooids that are mobilized are shown in gray, while buried ooids are white. **B**) The flow chart describes the specific steps of the program; *ooid (x)* represents the ooid at the top of column *x*.

number of time steps per velocity cycle. For columns greater than half the total number,

$$V(x) = \Delta V(X - x)\cos(2\pi t/t_c) \qquad (8)$$

where X is the total number of columns. This produces an increase in velocity toward the center of the model from each end (Fig. 5).

The top ooid in each column is mobilized if

$$r < |V(x)|^{3.45} \qquad (9)$$

where r is the unscaled radius of the ooid. The value of the exponent is the best-fit value for flume data relating water velocity 100 cm above the sediment surface to the threshold of sediment transport for grains < 2 mm in diameter (Miller et al. 1977, their fig. 6). According to Miller et al. (1977), grains with diameters > 2 mm can be transported when

$$r = const \cdot |V|^{2.22} \qquad (10)$$

The equation for small grain sizes (Eq 9) is used in the model, because new nuclei are considered to be < 2 mm in diameter. Also, the number of large ooids in any given run is much less than the number of small ooids, so possible differences in mobilization were ignored for simplicity. The model was also run with mobilization if $r \leq |V|^2$ for all ooids, and similar results were obtained.

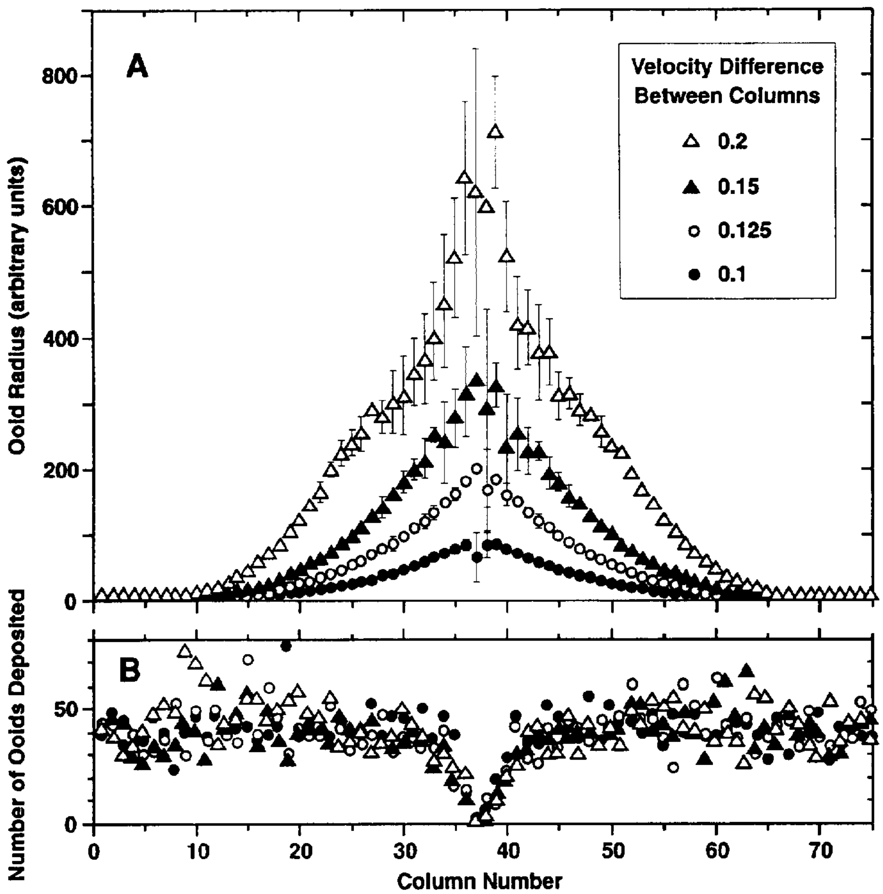

FIG 6.—A) Dependence of ooid radius on velocity gradient and location in the sorting model. Ooid size increases rapidly toward the center of the model, while the low-velocity ends contain uncoated nuclei. Average ooid size also increases with increasing velocity gradient and maximum velocity. Error bars represent 2σ in ooid size for each column and demonstrate the well sorted nature of the deposits at all but peak velocities. B) Number of ooids deposited in each column for data shown in part A. The number of ooids deposited in the central columns is extremely low for all velocity gradients and is the principal reason for the large variations in ooid size.

Once ooids that can be mobilized are identified, their radii are increased by the specified growth amount. Then they are transported one column in the direction of water flow and placed on top of all other ooids at that location. Mobilized ooids are transported to the right if the velocity is positive and to the left if it is negative. Only one ooid is mobilized per column. Because of the complexities of mixed-sized sediment transport, we limited the movement of mobile ooids to one column regardless of their ratio of size to water velocity. This is consistent with the observation that mixed-size bed load does not become strongly sorted during transport (Wilcock and Southard 1989).

The process is then repeated starting with introduction of nuclei. If no ooids are deposited in a column, the top ooid previously there is made available for mobilization during the next time step. Output consists of all ooids in the system, including some ooids at the tops of the columns that would be remobilized upon continued operation of the model.

Results.—The sorting model uses 75 columns, a growth rate of 1 unit per time step, an average of 7.5 nucleations per time step, ooid nuclei of 10 units, and 30,000 time steps for each run. Results are reported as ooid radius rather than as cortex thickness, because size is critical for mobilization of the ooids. Maximum ooid size is strongly dependent on magnitude and gradient of water velocity (Fig. 6A). With the velocity difference between columns set to 0.1, the maximum velocity is 3.7, producing a maximum ooid radius of about 80 units. The velocity gradient is low enough that ooids in the outer 20 columns are never mobilized but high enough that very few ooids are deposited in the central columns (Fig. 6B). The number of large ooids that can be deposited in the highest-velocity columns is limited by the lateral distance that a large ooid can be transported without being deposited in a lower-velocity column. As the velocity difference between columns increases, so does maximum ooid size, demonstrating that higher water velocity and velocity gradient can produce larger ooids.

Sorting becomes poorer with increasing water velocity, both at a set velocity gradient and between gradients. The small number of ooids deposited in high-velocity columns increases the influence of ooids that are only temporarily deposited in these columns and reduces the significance of the statistics. For steeper velocity gradients, the poorer sorting is also due to rapid fluctuations in velocity. In the central columns the velocity changes significantly between each time step, making the grain sizes that can be transported highly variable over short times. In a real system, velocity changes continuously and ooids are transported for variable distances; this might eliminate the poorer sorting observed in the model at higher velocities. The ooids are generally well sorted, however, and the model demonstrates one set of conditions that can produce deposits of well sorted, large ooids.

DISCUSSION

Utility of Results

Model results demonstrate that nuclei supply, growth rate, and agitation can all influence ooid size. Ooid nuclei supply can change rapidly, providing a mechanism for changing ooid size rapidly in a deposit. For example, many Precambrian oolites contain inversely graded beds of ooids. These may have formed because of an irregular supply of nuclei. A thin inversely graded bed could form if a single slug of ooid nuclei enters the system and then remains uncovered. Initially, the entire depth of the layer can be reworked and thus oolitically coated. As the ooids grow, more become permanently deposited, because of the inability of local processes to rework these larger ooids. Eventually, only ooids on the surface can be overturned and continue to grow without an increase in the agitation of the depositional environment. Because no new ooid nuclei enter the system, the older ooids are not buried. Eventually the ooids become too large to move, and they become cemented in place or more sediment enters the system. Changes like these are easiest to explain using changes in nucleation rate; they are unlikely to result from changes in growth rate, which should remain fairly constant over short time scales, or changes in ooid agitation, which are more likely to affect the larger-scale aspects of ooid deposition.

Changes in growth rate are difficult to identify, because increased growth rate may not leave a distinctive signature in the ooids or their arrangement. Growth rate might also be intimately linked to agitation and the delivery of fresh chemical species to the surfaces of the ooids. Thus, growth rate and agitation may not be independent, and distinguishing the influence of each in ancient oolites is extremely difficult.

Agitation is an interesting and complex process in ooid growth. In the growth model we account for daily processes by assuming that a certain thickness of ooids is continually reworked, and we specifically address only episodic, short-term erosional events. These events have no affect on ooid size because ooid growth is not enhanced during the event. In contrast, the sorting model requires an ooid to be mobilized before it can grow. Even if all ooids on the surface grew, enhanced growth of mobilized ooids makes ooid size dependent on the extent of reworking. It is thus critical to investigate the role of agitation in enhancing ooid growth.

Neoproterozoic Ooids

The relationships between ooid size on the one hand and nuclei supply, ooid growth rate, and agitation on the other hand provide a basis for evaluating conditions during the growth of Neoproterozoic giant ooids. Nuclei supply was probably lower in Neoproterozoic than in Phanerozoic time. The major sources of ooid nuclei are skeletal fragments, fecal pellets, and eroded grains (Bathurst 1975). Lack of fecal pellets and skeletal fragments in Archean and Proterozoic time suggests that supply of ooid nuclei prior to the evolution of metazoans might have been lower. It is unlikely, however, that a low nuclei supply was the sole cause of the giant ooids in Neoproterozoic rocks. If the number of ooid nuclei was limited by the absence of fecal pellets and skeletal fragments, the shortage of ooid nuclei should have been approximately constant throughout Archean and Proterozoic time, and large ooids should have been common at all times prior to the evolution of metazoans, not just in Neoproterozoic deposits. Thus, we suspect that lack of nuclei was not the dominant factor leading to the growth of Neoproterozoic giant ooids.

Two of the major variables affecting growth rate are carbonate saturation state of sea water and kinetic factors either promoting or inhibiting carbonate precipitation. Both of these may have changed significantly over time (Grotzinger 1989; Tucker 1992). Little is known, however, about absolute growth rates in modern times, and even less is known about past growth rates.

Numerous kinetic factors make estimating growth rate of modern ooids difficult. In one of the few studies of carbonate precipitation rates, Weyl (1967) measured precipitation rates on natural ooids in modern sea water by passing ocean water through a U-tube filled with ooids and measuring volume of sea water, changes in pH, and surface area of the ooids. From this he obtained an approximate steady-state precipitation rate of 5×10^{-5} nm/s on the ooids. This is equivalent to a growth rate of 1.6 mm/ky. If this rate is of the right order of magnitude, 2000 years of active growth time would be necessary to precipitate a 3 mm oolitic coating, excluding time when the ooid is temporarily deposited and does not grow. If growth of Neoproterozoic giant ooids had been this slow, sediment accumulation rates would have been an order of magnitude lower than the subsidence rates of most platforms (1–10 cm/ky; Schlager 1981) and the platforms would have drowned. This suggests that either the rate Weyl (1967) measured is much lower than the actual modern ooid growth rate or growth rates were much higher when giant ooids formed.

One important factor that could increase the effective rate of modern ooid growth over that measured by Weyl (1967) is enhancement of precipitation in agitated environments. Both empirical and theoretical evidence suggests that agitation increases precipitation rates through constant delivery of chemically undepleted water and through degassing of carbon dioxide (Bathurst 1975). Even taking these two effects into consideration, increased growth rates may still be needed to form giant ooids.

Growth rate of abiotic carbonate could have been higher before the advent of carbonate-secreting organisms (Swett and Knoll 1989), because abiotic carbonate must have been the dominant carbonate sink in Precambrian oceans. This does not explain the predominance of giant ooids in Neoproterozoic deposits. Archean and Paleoproterozoic carbonate platforms contain anomalously high proportions of marine cements, and the proportion of marine cement decreases through Mesoproterozoic and Neoproterozoic time (Grotzinger 1989; Grotzinger and Kasting 1993). This suggests that precipitation was not faster in Neoproterozoic time than in the rest of Precambrian time and leads to the conclusion that high rate of inorganic precipitation is not the main cause of the deposits of giant ooids in Neoproterozoic carbonates. High ooid growth rates can thus be eliminated as the dominant factor in the growth of Neoproterozoic giant ooids.

While little is understood about the growth of ooids and circumstances leading to their ultimate deposition, it is clear that large ooids require at least episodically high water velocity to grow symmetrically. High water velocity may also enhance the growth of ooids through the chemical and physical processes discussed above. Well sorted deposits of large ooids require high water velocity either to transport the large ooids or to winnow out smaller grains. These considerations imply that high water velocity is important for extensive deposits of giant ooids.

An increase in the environmental energy of Neoproterozoic platforms could have influenced the formation of giant ooids. Agitation may have been greater because of the predominance of carbonate ramps over rimmed carbonate platforms (Grotzinger 1989) due to a decline in reef-forming stromatolites during Neoproterozoic time (Grotzinger 1990). Because ramps are less protected from open-ocean waves and tidal currents than are other platform geometries, an increase in the number of ramps relative to other kinds of platforms should increase the average energy of carbonate depositional environments (Logan et al. 1969; Osleger 1991). The presence of more carbonate ramps in the Neoproterozoic could have led to higher average water velocities and thus to abundant deposits of large ooids. The reason that giant ooids are not present in modern high-energy carbonate platforms might be that the abundant supply of biologically produced nuclei and low ooid growth rate limit ooid size. In view of the lower nucleation rate and higher growth rate during Neoproterozoic time, however, environmental energy conditions may have been the main control on Neoproterozoic deposits of giant ooids.

CONCLUSIONS

Results from the ooid growth model and sorting model suggest that: (1) Lower ooid nuclei supply increases average ooid size. (2) Increased growth rate leads to larger ooids even though the number of oolitic coatings decreases due to earlier burial. (3) Storm reworking of deposited ooids does not affect ooid size, because growth is not enhanced during the erosional event. (4) Higher water velocity and velocity gradient tend to increase ooid size if mobilization enhances ooid growth. In addition, velocity gradients produce well sorted deposits and concentrate the largest ooids.

Neoproterozoic giant ooids may have formed through a combination of lower nuclei supply, higher growth rate, and higher average agitation level: (1) Lack of fecal pellets and skeletal fragments during Precambrian time might have lowered nucleation rates sufficiently to increase average ooid diameter, but this would have promoted giant ooid growth not only in Neoproterozoic deposit, but throughout Precambrian time. (2) Ooid growth rate may have been higher during Neoproterozoic time, but there is little evidence that the abiotic carbonate precipitation rate was higher than in the rest of Precambrian time. (3) An increase in average water velocity in carbonate depositional environments due to a predominance of ramps over rimmed shelves in Neoproterozoic time may have promoted the growth of giant ooids.

ACKNOWLEDGMENTS

This work was supported by a National Science Foundation Graduate Fellowship to DYS and by NASA Grant #NAGW-2795 to JPG. The authors would like to thank Peter S. Kaufman and Linda C. Kah for their extensive participation at the beginning of the project. In addition, reviews from Bruce H. Wilkinson, David Osleger, Mark R. Boardman, and John B. Southard provided direction for greatly improving the presentation of this research.

REFERENCES

Amsden, T.W., and Barrick, J.E., 1986, Late Ordovician–Early Silurian strata in the central United States and the Hirnantian Stage: Oklahoma Geological Survey Bulletin 139, 97 p.

Bathurst, R.G.C., 1975, Carbonate Sediments and Their Diagenesis: Developments in Sedimentology 12, Amsterdam, Elsevier, 658 p.

Beukes, N.J., 1983, Ooids and oolites of the Proterophytic Boomplaas Formation, Transvaal Supergroup, Griqualand West, South Africa, *in* Peryt, T.M., ed., Coated Grains: Berlin, Springer-Verlag, p. 199–214.

Blodgett, R.B., Clough, J.G., Dutro, J.T.J., Ormiston, A.R., Palmer, A.R., and Taylor, M.E., 1986, Age revisions for the Nanook Limestone and Katakturuk Dolomite, northeastern Brooks Range, *in* Bartsch-Winkler, S., and Reed, K.M., eds., Geologic Studies in Alaska by the U.S. Geological Survey During 1985: United States Geological Survey Circular 978, p. 5–10.

Carozzi, A.V., 1989, Carbonate Rock Depositional Modes: A Microfacies Approach: Englewood Cliffs, New Jersey, Prentice-Hall, 604 p.

Ciarapica, G., and Passeri, L., 1983, Coated grains in contrasted environmental situations: Norian and Lower Liassic of northern Apennines, *in* Peryt, T.M., ed., Coated Grains: Berlin, Springer-Verlag, p. 576–586.

Clough, J.G., Blodgett, R.B., Imm, T.A., and Pavia, E.A., 1988, Depositional environments of the Katakturuk Dolomite and Nanook Limestone, Arctic National Wildlife Refuge, Alaska (abstract): American Association of Petroleum Geologists Bulletin, Abstracts, v. 72, p. 172.

Davies, P.J., Bubela, B., and Ferguson, J., 1978, The formation of ooids: Sedimentology, v. 25, p. 703–730.

Grotzinger, J.P., 1989, Facies and evolution of Precambrian carbonate depositional systems: emergence of the modern platform archetype, *in* Crevello, P.D., Wilson, J.L., Sarg, J.F., and Read, J.F., eds., Controls on Carbonate Platform and Basin Development: SEPM Special Publication 44, p. 79–106.

Grotzinger, J.P., 1990, Geochemical model for Proterozoic stromatolite decline: American Journal of Science, v. 290-A, p. 80–103.

Grotzinger, J.P., and Kasting, J.F., 1993, New constraints on Precambrian ocean composition: Journal of Geology, v. 101, p. 237–245.

Grotzinger, J.P., and Read, J.F., 1983, Evidence for primary aragonite precipitation, lower Proterozoic (1.9 Ga) dolomite, Wopmay orogen, northwest Canada: Geology, v. 11, p. 710–713.

Gutstadt, A.M., 1968, Petrology and depositional environments of the Beck Spring Dolomite (Precambrian), Kingston Range, California: Journal of Sedimentary Petrology, v. 38, p. 1280–1289.

Hall, W.D.M., and Goode, A.D.T., 1978, The early Proterozoic Nabberu Basin and associated iron formations of western Australia: Precambrian Research, v. 7, p. 129–184.

Heller, P.L., Komar, P.D., and Pevear, D.R., 1980, Transport processes in ooid genesis: Journal of Sedimentary Petrology, v. 50, p. 943–952.

King, D.T.J., and Chafetz, H.S., 1983, Tidal-flat to shallow-shelf deposits in the Cap Mountain Limestone member of the Riley Formation, Upper Cambrian of central Texas: Journal of Sedimentary Petrology, v. 53, p. 261–273.

Knoll, A.H., and Swett, K., 1990, Carbonate deposition during the later Proterozoic Era: an example form Spitsbergen: American Journal of Science, v. 290-A, p. 104–132.

Logan, B.W., Harding, J.L., Ahr, W.M., Williams, J.B., and Snead, R.G., 1969, Carbonate Sediments and Reefs, Yucatan Shelf, Mexico: American Association of Petroleum Geologists Memoir 11, 198 p.

Markello, J.R., and Read, J.F., 1981, Carbonate ramp-to-deeper shale shelf transitions of an Upper Cambrian intrashelf basin, Nolichucky Formation, southwest Virginia Appalachians: Sedimentology, v. 28, p. 573–597.

Medwedeff, D.A., and Wilkinson, B.H., 1983, Cortical fabrics in calcite and aragonite ooids, *in* Peryt, T.M., ed., Coated Grains: Berlin, Springer-Verlag, p. 109–115.

Miller, M.C., McCave, I.N., and Komar, P.D., 1977, Threshold of sediment motion under unidirectional currents: Sedimentology, v. 24, p. 507–527.

Milliman, J.D., and Barretto, H.T., 1975, Relict magnesian calcite oolite and subsidence of the Amazon Shelf: Sedimentology, v. 22, p. 137–145.

Osleger, D., 1991, Subtidal carbonate cycles: implications for allocyclic vs. autocyclic controls: Geology, v. 19, p. 917–920.

Peryt, T.M., 1983, Classification of coated grains, *in* Peryt, T.M., ed., Coated Grains: New York, Springer-Verlag, p. 3–6.

Press, W.H., Flannery, B.P., Teukolsky, S.A., and Vetterling, W.T., 1988, Numerical Recipes in C: The Art of Scientific Computing: New York, Cambridge University Press, 735 p.

Reijers, T.J.A., and ten Have, A.H.M., 1983, Ooid zonation as indication for environmental conditions in a Givetian–Frasnian carbonate shelf-slope transition, *in* Peryt, T.M., ed., Coated Grains: New York, Springer-Verlag, p. 188–198.

Richter, D.K., 1983, Calcareous ooids: a synopsis, *in* Peryt, T.M., ed., Coated Grains: New York, Springer-Verlag, p. 71–99.

Sandberg, P.A., 1983, An oscillating trend in Phanerozoic non-skeletal carbonate mineralogy: Nature, v. 305, p. 19–22.

Sandberg, P.A., 1985, Nonskeletal aragonite and pCO_2 in the Phanerozoic and Proterozoic, *in* Sundquist, E.T., and Broecker, W.S., eds., The Carbon Cycle and Atmospheric CO_2: Natural Variations Archean to Present: American Geophysical Union, Geophysical Monograph 32, p. 585–594.

Schlager, W., 1981, The paradox of drowned reefs and carbonate platforms: Geological Society of America Bulletin, v. 92, p. 197–211.

Simonson, B.M. and Jarvis, D.G., in press, Microfabrics of oolites and pisolites in the 2.5 Ga Carawine Dolomite of western Australia, *in* Rezak, R., and Lavoie, D., eds., Carbonate Microfabrics: Berlin, Springer-Verlag.

Simonson, B.M., Schubel, K.A., and Hassler, S.W., 1993, Carbonate sedimentology of the early Precambrian Hamersley Group of Western Australia: Precambrian Research, v. 60, p. 287–337.

Singh, U., 1987, Ooids and cements from the late Precambrian of the Flinders Ranges, South Australia: Journal of Sedimentary Petrology, v. 57, p. 117–127.

Sorby, H.C., 1879, Anniversary address of the president: Proceedings Quarterly Journal of the Geological Society of London, v. 35, p. 56–95.

Southgate, P.N., 1989, Relationships between cyclicity and stromatolite form in the Late Proterozoic Bitter Springs Formation, Australia: Sedimentology, v. 36, p. 323–339.

Swett, K., and Knoll, A.H., 1989, Marine pisolites from Upper Proterozoic carbonates of East Greenland and Spitsbergen: Sedimentology, v. 36, p. 75–93.

Teitz, M., and Mountjoy, E.W., 1989, The late Proterozoic Yellowhead carbonate platform west of Jasper, Alberta, *in* Geldsetzer, H.H.J., James, N.P., and Tebbutt, G.E., eds., Reefs, Canada and Adjacent Area: Canadian Society of Petroleum Geologists Memoir 13, p. 129–134.

Truswell, J.F., and Eriksson, K.A., 1973, Stromatolitic associations and their palaeo-environmental significance: a re-appraisal of a lower Proterozoic locality from the northern Cape Province, South Africa: Sedimentary Geology, v. 10, p. 1–23.

Tucker, M.E., 1984, Calcitic, aragonitic and mixed calcitic-aragonitic ooids from the mid-Proterozoic Belt Supergroup, Montana: Sedimentology, v. 31, p. 627–644.

Tucker, M.E., 1992, The Precambrian–Cambrian boundary: seawater chemistry, ocean circulation and nutrient supply in metazoan evolution, extinction and biomineralization: Geological Society of London Journal, v. 149, p. 655–668.

Weyl, P.K., 1967, The solution behavior of carbonate materials in sea water: University of Miami Studies in Tropical Oceanography, v. 5, p. 178–228.

Wilcock, P.R., and Southard, J.B., 1989, Bed load transport of mixed size sediment: fractional transport rates, bed forms, and the development of a coarse bed surface layer: Water Resources Research, v. 25, p. 1629–1641.

Wilkinson, B.H., Buczynski, C., and Owen, R.M., 1984, Chemical control of carbonate phases; implications from Upper Pennsylvanian calcite-aragonite ooids of southeastern Kansas: Journal of Sedimentary Petrology, v. 54, p. 932–947.

Wilkinson, B.H., Owen, R.M., and Carroll, A.R., 1985, Submarine hydrothermal weathering, global eustasy, and carbonate polymorphism in Phanerozoic marine oolites: Journal of Sedimentary Petrology, v. 55, p. 171–183.

Received 22 January 1993; accepted 30 March 1993.

LIST OF VARIABLES

General Variables

r	radius of ooid
t	time
$\Delta m_{abrasion}$	mass loss due to abrasion
F_{impact}	force of impact between ooids
K	factor relating actual mass loss to impact force
a	deceleration of ooid during impact
ρ	density of ooid
I	number of impacts
Δm_{growth}	ooid mass increase from growth

Growth-Model Variables

f	frequency of storm reworking
D	depth of exhumation for a particular storm
λ	exhumation parameter
R	random number between 0 and 1
D_{growth}	depth to base of growth bin
D_{max}	depth to base of deposition bin

Sorting-Model Variables

P	probability for a column to recieve an ooid nucleus
N	average number of nuclei added each time step
X	total number of columns
ΔV	water velocity difference between columns
x	column number
$V(x)$	water velocity at column x
t_c	number of time steps for each velocity cycle